



**HAL**  
open science

# Walking in a Planar Poisson-Delaunay Triangulation: Shortcuts in the Voronoi Path

Olivier Devillers, Louis Noizet

► **To cite this version:**

Olivier Devillers, Louis Noizet. Walking in a Planar Poisson-Delaunay Triangulation: Shortcuts in the Voronoi Path. *International Journal of Computational Geometry and Applications*, 2018, 28 (3), pp.255-269. 10.1142/S0218195918500061 . hal-01712628

**HAL Id: hal-01712628**

**<https://inria.hal.science/hal-01712628v1>**

Submitted on 19 Feb 2018

**HAL** is a multi-disciplinary open access archive for the deposit and dissemination of scientific research documents, whether they are published or not. The documents may come from teaching and research institutions in France or abroad, or from public or private research centers.

L'archive ouverte pluridisciplinaire **HAL**, est destinée au dépôt et à la diffusion de documents scientifiques de niveau recherche, publiés ou non, émanant des établissements d'enseignement et de recherche français ou étrangers, des laboratoires publics ou privés.

# Walking in a Planar Poisson-Delaunay Triangulation: Shortcuts in the Voronoi Path\*

Olivier Devillers<sup>†</sup>      Louis Noizet<sup>‡</sup>

Université de Lorraine, CNRS, Inria, LORIA, F-54000 Nancy, France.

## Abstract

Let  $X_n$  be a planar Poisson point process of intensity  $n$ . We give a new proof that the expected length of the Voronoi path between  $(0,0)$  and  $(1,0)$  in the Delaunay triangulation associated with  $X_n$  is  $\frac{4}{\pi} \simeq 1.27$  when  $n$  goes to infinity; and we also prove that the variance of this length is  $\Theta(1/\sqrt{n})$ . We investigate the length of possible shortcuts in this path, and define a shortened Voronoi path whose expected length can be expressed as an integral that is numerically evaluated to  $\simeq 1.16$ . The shortened Voronoi path has the property to be *locally defined*; and is shorter than the previously known locally defined paths in Delaunay triangulation such as the upper path whose expected length is  $35/3\pi^2 \simeq 1.18$ .

## 1 Introduction

The Delaunay triangulation is one of the most classical objects of computational geometry and searching for paths in a point set using Delaunay edges is useful, e.g. for point location, nearest neighbor search,[10] or routing in networks.[3]

If the points are random, several walking strategies have been studied.[2, 4, 7, 8, 11] In this paper we consider variations of a particular strategy called the *Voronoi path* that consists in linking in order all the nearest neighbors of a point moving linearly from  $s$  to  $t$  where  $s$  and  $t$  are two points in the plane. We analyze this path when  $[st]$  is a fixed segment of unit length and when the point set is a Poisson point process of density  $n$ , possibly augmented by the two points  $s$  and  $t$ .

The Voronoi path is known to have an expected length  $\frac{4}{\pi} \simeq 1.27$  when  $n \rightarrow \infty$ . [1] In this paper, we provide an alternative proof of this result (Section 3) and prove that this length is quite stable by showing that its variance is small (Section 4).

A path is called *locally defined* if it is possible to decide if an edge  $e$  belongs to the path from  $s$  to  $t$  knowing only  $s$ ,  $t$ ,  $e$ , and the neighbors of the endpoints of  $e$  (without knowing the rest of the path). Clearly, the Voronoi path is locally defined, since it can be decided if a Delaunay edge  $e$  belongs to the Voronoi path by testing if the dual Voronoi edge of  $e$  crosses the segment  $[st]$ . Another locally defined path is the *upper path*[7] whose expected length,  $\frac{35}{3\pi^2} \simeq 1.182$ , is shorter than the Voronoi path. In Section 5 we introduce a variant of the Voronoi path using some locally defined shortcuts. The expected length of this improved path can be expressed as an integral whose numerical evaluation yields an expected length of 1.16, and thus give a shorter locally defined path.

## 2 Notation, Definitions, and Preliminaries

For a point set  $\chi$  in the plane, we define its Delaunay triangulation  $\text{Del}(\chi)$  as the set of edges  $[pq]$  with  $p, q \in \chi$  such that there exists a disk  $D$  with  $D \cap \chi = \{p, q\}$ . One can remark that if such a disk exists, there

---

\*This work has been partially supported by ANR Projects Presage (ANR-11-BS02-003) and ASPAG (ANR-17-CE40-0017)

<sup>†</sup>[members.loria.fr/Olivier.Devillers/](http://members.loria.fr/Olivier.Devillers/)

<sup>‡</sup><http://louis.noizet.fr/>

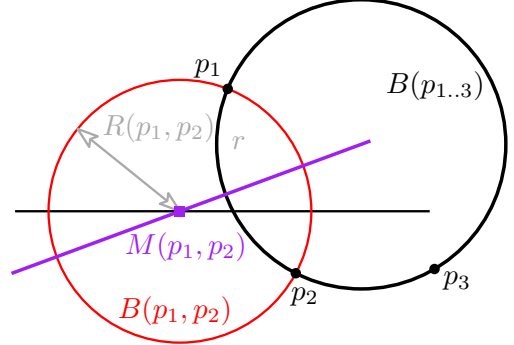
is also an empty disk with  $p$  and  $q$  on its boundary (shrink the first disk staying inside to reach the relevant configuration).

The Voronoi diagram associated with  $\chi$  is the tuple  $(R_i)_{i \in \chi}$  where  $\forall p \in \chi; R_p = \{q \in \mathbb{R}^2 / \forall p' \in \chi \|pq\| \leq \|p'q\|\}$  (with  $\|\cdot\|$  the Euclidean norm).  $R_p$  is the Voronoi cell of seed  $p$ . If  $[pq]$  is a Delaunay edge, then the Voronoi cells of  $p$  and  $q$  are neighbors and  $R_p \cap R_q$  is called the dual Voronoi edge.

The *Voronoi path*  $VP_\chi(s, t)$  between two points  $s$  and  $t$  is defined as the path formed by the seeds of the Voronoi cells intersecting the segment  $[st]$  (see Figure 1 for an example of Voronoi path). If  $s, t \in \chi$  this path links  $s$  to  $t$ , otherwise it links the nearest neighbor of  $s$  to the nearest neighbor of  $t$ .

We use the notation  $p_{1..i}$  for the tuple of  $i$  points  $(p_1, \dots, p_i)$  and  $p_{1 \neq i}$  for same tuples without duplicates, i.e. when  $\forall k, l \in [1, i], p_k \neq p_l$ .

We denote by  $M(p_1, p_2)$  the intersection point between the bisector of two points  $p_1$  and  $p_2$  and the line  $(st)$ . The ball centered at  $M(p_1, p_2)$  passing through  $p_1$  and  $p_2$  is denoted  $B(p_1, p_2)$  and its radius is denoted  $R(p_1, p_2)$ . The ball passing through  $p_1, p_2$ , and  $p_3$  is denoted  $B(p_{1..3})$ .



A ball with center  $(x, 0)$  and radius  $r$  is denoted  $B(x, r)$ . The area of a domain  $D$  is denoted  $\mathcal{A}(D)$ .

In the sequel our point set will be a Poisson point process  $X_n$  of intensity  $n$  or the same set augmented by two points  $X = X_n \cup \{s, t\}$  where  $s = (0, 0)$  and  $t = (1, 0)$ .

For a random variable  $Y$ , its expected value is denoted  $\mathbb{E}[Y]$  and its variance is denoted  $\mathbb{V}[Y]$ . The probability of an event  $Z$  is denoted  $\mathbb{P}[Z]$ .

We recall the Slivnyak-Mecke formula which allows one to transform a sum on a Poisson point process in an integral. For a function  $f$  computing a real value from a set of points distributed according Poisson distribution, we have:[12, Theorem 3.3.5]

$$\mathbb{E} \left[ \sum_{p_1 \neq \dots, k \in X_n^k} f(X_n) \right] = \mathbb{E} \left[ \int f(X_n \cup \{p_{1..k}\}) dp_{1..k} \right]$$

We recall the Blaschke-Petkantschin change of variable which substitutes to the Cartesian coordinates of three points  $p_{1..3}$  their circumscribing circle of center  $\Omega$  and radius  $r$  and the polar angles of the three points  $\alpha_{1..3}$  on that circle. For a function  $f$  of the three points, we have:[12, Theorem 7.3.1]

$$\int_{\mathbb{R}^2} \int_{\mathbb{R}^2} \int_{\mathbb{R}^2} f(p_{1..3}) dp_{1..3} = \int_{[0, 2\pi]^3} \int_0^\infty \int_{\mathbb{R}} \int_{\mathbb{R}} f(\Omega, r, \alpha_{1..3}) 2r^3 \mathcal{A}(\alpha_{1..3}) dy_\Omega dx_\Omega dr d\alpha_{1..3},$$

### 3 Expected Length of the Voronoi Path

The first theorem proves that the length of the Voronoi path in  $X$  and  $X_n$  are similar when  $n$  is big:

**Theorem 1.** *Let  $X := X_n \cup \{s, t\}$  where  $X_n$  is a planar Poisson point process of intensity  $n$ ,  $s = (0, 0)$ , and  $t = (1, 0)$ . Let  $\ell(VP_X(s, t))$  be the length of the Voronoi Path from  $s$  to  $t$  in  $\text{Del}(\chi)$ . Then*

$$\left| \mathbb{E}[\ell(VP_X(s, t))] - \mathbb{E}[\ell(VP_{X_n}(s, t))] \right| = O\left(\frac{1}{\sqrt{n}}\right)$$

*Proof.* First, we remark that with very high probability  $1 - e^{-n\frac{\pi}{4}}$ , the disk of diameter  $[st]$  contains at least one point of  $X_n$  and thus no disk centered on  $[st]$  can contain both  $s$  and  $t$ .

If no disk contains both  $s$  and  $t$ ,  $VP_X(s, t)$  and  $VP_{X_n}(s, t)$  only differ by few edges around  $s$  and around  $t$ . Actually, when adding  $s$  and  $t$  to  $X_n$  and updating the Voronoi diagram, the Voronoi cell of  $s$

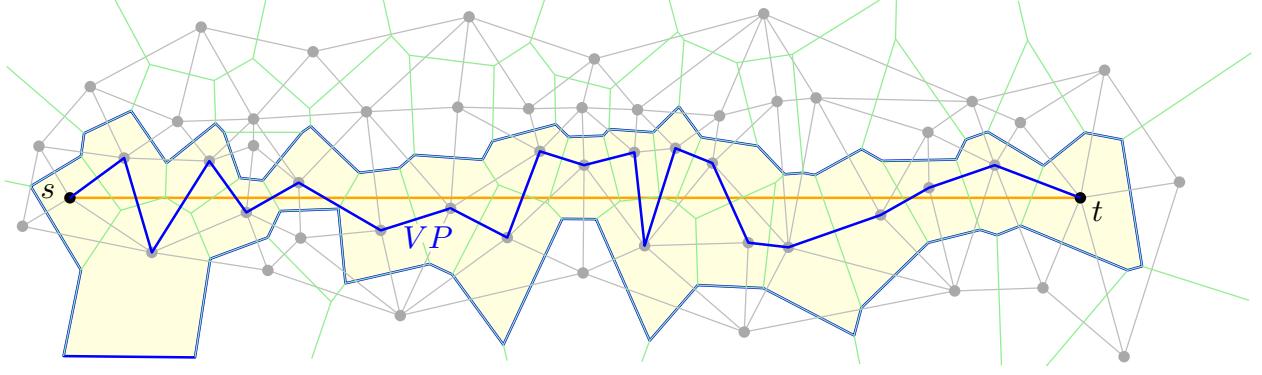


Figure 1: The Voronoi path

and  $t$  are created and the parts of segment  $[st]$  inside these new cells induce changes between  $VP_X(s, t)$  and  $VP_{X_n}(s, t)$ . Namely, if we denote by  $q_1, q_2, \dots, q_{k-1}, q_k$  the vertices of  $VP_{X_n}(s, t)$ , then  $VP_X(s, t)$  is  $s, q_i, q_{i+1}, \dots, q_{j-1}, q_j, t$  for some values  $i$  and  $j$  such that  $1 \leq i \leq j \leq k$ . We remark that all  $q_l$ , for  $1 \leq l \leq i$ , are neighbors of  $s$  in  $\text{Del}(X)$  since, by definition of the paths, there is a disk  $D_l$  centered on a point in  $[st]$  with  $q_l$  on its boundary,  $s$  inside and no points of  $X_n$  nor  $t$  inside. this disk witnesses that  $[sq_l]$  is a Delaunay edge in  $\text{Del}(X)$ . Thus, to go from  $VP_{X_n}(s, t)$  to  $VP_X(s, t)$  we have to add one Delaunay edge incident to  $s$ :  $[sq_i]$  and to remove few edges between neighbors of  $s$  in  $\text{Del}(X)$ . The length variation at the beginning of the path can be bounded using triangular inequality by:

$$\|q_1q_2\| + \|q_2q_3\| + \dots + \|q_{i-1}q_i\| + \|sq_i\| \leq \|sq_1\| + 2\|sq_2\| + 2\|sq_3\| + \dots + 2\|sq_{i-1}\| + 2\|sq_i\|$$

whose expectation is  $O\left(\frac{1}{\sqrt{n}}\right)$ . [7, Prop. 2.2] The same applies to the end of the path around  $t$ .

In the rare case with an empty disk of diameter  $[st]$  almost the same reasoning applies except that the two parts of  $VP_{X_n}(s, t)$  to be removed may overlap. The length of the removed part is still bounded from above by  $O\left(\frac{1}{\sqrt{n}}\right)$ . Now the added part is just edge  $st$  of length one, but since it arises only with probability  $e^{-n\frac{\pi}{4}} = o\left(\frac{1}{\sqrt{n}}\right)$  the result still holds.  $\square$

**Theorem 2.** *Under the same hypotheses as Theorem 1, we have*

$$\mathbb{E}[\ell(VP_{X_n}(s, t))] = \frac{4}{\pi}.$$

*Proof.* The length of the Voronoi path is expressed as a sum on all pairs of points using indicator functions:

$$\begin{aligned} \ell(VP_{X_n}(s, t)) &= \frac{1}{2} \sum_{p_1 \neq p_2 \in X_n^2} \mathbb{1}_{[p_1p_2] \in VP_{X_n}(s, t)} \|p_2p_1\| \\ &= \frac{1}{2} \sum_{p_1 \neq p_2 \in X_n^2} \mathbb{1}_{[M(p_1, p_2) \in [st]]} \mathbb{1}_{[B(p_1, p_2) \cap X_n = \emptyset]} \|p_2p_1\|. \end{aligned}$$

Using the Slivnyak-Mecke formula, we transform this sum in an integral:

$$\mathbb{E}[\ell(VP_{X_n}(s, t))] = \frac{n^2}{2} \int_{(\mathbb{R}^2)^2} \mathbb{1}_{[M(p_1, p_2) \in [st]]} \mathbb{P}[B(p_1, p_2) \cap X_n = \emptyset] \|p_2p_1\| dp_{1,2}.$$

This integral will be computed by substitution. Let  $\Phi$  be the function

$$\begin{aligned} \Phi : \mathbb{R} \times \mathbb{R}_{\geq 0} \times [0, 2\pi]^2 &\longrightarrow \mathbb{R}^2 \times \mathbb{R}^2 \\ (x, r, \alpha_1, \alpha_2) &\longmapsto (p_1, p_2), \end{aligned}$$

where for  $i=1,2$  we let  $p_i = (x, 0) + r(\cos \alpha_i, \sin \alpha_i)$ . As long as  $p_1$  and  $p_2$  do not have the same abscissa, which occurs with probability 1, the predecessor of  $(p_1, p_2)$  by  $\Phi$  is uniquely defined, with  $x$  is the abscissa of  $M(p_1, p_2)$  and  $r$  is the distance between this point and  $p_1$ . So  $\Phi$  is a  $C^1$ -diffeomorphism up to a null set. Its Jacobian is

$$\det(J_\Phi) = \begin{vmatrix} 1 & \cos \alpha_1 & -r \sin \alpha_1 & 0 \\ 0 & \sin \alpha_1 & r \cos \alpha_1 & 0 \\ 1 & \cos \alpha_2 & 0 & -r \sin \alpha_2 \\ 0 & \sin \alpha_2 & 0 & r \cos \alpha_2 \end{vmatrix} = r^2(\cos \alpha_2 - \cos \alpha_1).$$

Since  $\|p_1 p_2\| = 2r \left| \sin \frac{\alpha_1 - \alpha_2}{2} \right|$  and  $\mathbb{P}[\mathbb{B}(0, r) \cap X_n = \emptyset] = e^{-n\pi r^2}$ , we get

$$\begin{aligned} &\mathbb{E}[\ell(VP_{X_n}(s, t))] \\ &= \frac{n^2}{2} \int_{-\infty}^{\infty} \int_0^{\infty} \int_{[0, 2\pi]^2} \mathbb{1}_{[0 < x < 1]} e^{-n\pi r^2} 2r \left| \sin \frac{\alpha_1 - \alpha_2}{2} \right| \cdot |\det(J_\Phi)| d\alpha_1 d\alpha_2 dr dx \\ &= n^2 \int_{-\infty}^{\infty} \mathbb{1}_{[0 < x < 1]} dx \int_0^{\infty} e^{-n\pi r^2} r^3 dr \int_{[0, 2\pi]^2} \left| \sin \frac{\alpha_1 - \alpha_2}{2} \right| \cdot |\cos \alpha_2 - \cos \alpha_1| d\alpha_1 d\alpha_2 \quad (1) \\ &= n^2 \cdot 1 \cdot \frac{1}{2\pi^2 n^2} \cdot 4 \int_0^\pi \int_{\alpha_2}^{2\pi - \alpha_2} \sin \frac{\alpha_1 - \alpha_2}{2} (\cos \alpha_2 - \cos \alpha_1) d\alpha_1 d\alpha_2 \\ &= n^2 \frac{1}{2\pi^2 n^2} \cdot 4 \cdot 2\pi = \frac{4}{\pi}, \end{aligned}$$

using the fact that  $\left| \sin \frac{\alpha_1 - \alpha_2}{2} \right| \cdot |\cos \alpha_2 - \cos \alpha_1|$  is invariant by substituting  $(\alpha_2, \alpha_1)$  or  $(2\pi - \alpha_1, 2\pi - \alpha_2)$  to  $(\alpha_1, \alpha_2)$ .  $\square$

## 4 Variance of Stretch Factor of the Voronoi Path

**Theorem 3.** *Under the same hypotheses as Theorem 1, the variance verifies*

$$\mathbb{V}[\ell(VP_{X_n})] = \Theta(n^{-\frac{1}{2}}).$$

*Proof.* The variance is given by:

$$\mathbb{V}[\ell(VP_{X_n})] = \mathbb{E}[\ell(VP_{X_n})^2] - \mathbb{E}[\ell(VP_{X_n})]^2.$$

We define  $\ell_{VP}(p_{1..2}) = \mathbb{1}_{[B(p_1, p_2) \cap X_n = \emptyset]} \mathbb{1}_{[M(p_1, p_2) \in [st]]} \|p_1 p_2\|$  and develop  $\ell(VP_{X_n})^2$  as a sum:

$$\begin{aligned}
\ell(VP_{X_n})^2 &= \left( \frac{1}{2} \sum_{p_1 \neq, 2 \in X_n^2} \ell_{VP}(p_{1..2}) \right)^2 \\
&= \frac{1}{4} \left( 2 \sum_{p_1 \neq, 2 \in X_n^2} \ell_{VP}(p_{1..2})^2 \right) \\
&\quad + \frac{1}{4} \left( 4 \sum_{p_1 \neq, 3 \in X_n^3} \ell_{VP}(p_{1..2}) \ell_{VP}(p_{2..3}) \right) \\
&\quad + \frac{1}{4} \left( \sum_{p_1 \neq, 4 \in X_n^4} \ell_{VP}(p_{1..2}) \ell_{VP}(p_{3..4}) \right). \tag{2}
\end{aligned}$$

The expected value of the three terms of Equation (2) will be computed separately using the same technique as for Theorem 2. The last term gives, with  $X' = X_n \cup \{p_{1..4}\}$ :

$$\begin{aligned}
&\mathbb{E} \left[ \frac{1}{4} \sum_{p_1 \neq, 4 \in X_n^4} \ell_{VP_{X_n}}(p_{1..2}) \ell_{VP_{X_n}}(p_{3..4}) \right] \\
&= \frac{n^4}{4} \int_{(\mathbb{R}^2)^4} \mathbb{E} [\ell_{VP_{X'}}(p_{1..2}) \ell_{VP_{X'}}(p_{3..4})] dp_{1..4}. \\
&= \frac{n^4}{4} \int_{(\mathbb{R}^2)^4} \mathbb{E} [\mathbb{1}_{[B(p_1, p_2) \cap X' = \emptyset]} \mathbb{1}_{[B(p_3, p_4) \cap X' = \emptyset]}] \mathbb{1}_{[M(p_1, p_2) \in [st]]} \\
&\quad \mathbb{1}_{[M(p_3, p_4) \in [st]]} \|p_1 p_2\| \|p_3 p_4\| dp_{1..4} \\
&\leq \frac{n^4}{4} \int_{(\mathbb{R}^2)^4} \mathbb{E} [\mathbb{1}_{[B(p_1, p_2) \cap X_n = \emptyset]} \mathbb{1}_{[B(p_3, p_4) \cap X_n = \emptyset]}] \mathbb{1}_{[M(p_1, p_2) \in [st]]} \\
&\quad \mathbb{1}_{[M(p_3, p_4) \in [st]]} \|p_1 p_2\| \|p_3 p_4\| dp_{1..4}.
\end{aligned}$$

With the same substitution as previously, done twice, we get:

$$\begin{aligned}
&\mathbb{E} \left[ \frac{1}{4} \sum_{p_1 \neq, 4 \in X_n^4} \ell_{VP_{X_n}}(p_{1..2}) \ell_{VP_{X_n}}(p_{3..4}) \right] \\
&\leq \frac{n^4}{4} \int_{[0,1]^2} \int_{\mathbb{R}_{\geq 0}^2} \int_{[0, 2\pi]^4} e^{-n \mathcal{A}(B(x, r) \cup B(x', r'))} 2r |\sin \frac{\alpha_1 - \alpha_2}{2}| 2r' |\sin \frac{\alpha_3 - \alpha_4}{2}| \\
&\quad r^2 |\cos \alpha_2 - \cos \alpha_1| r'^2 |\cos \alpha_4 - \cos \alpha_3| d\alpha_{1..4} dr dr' dx dx'.
\end{aligned}$$

By rewriting the exponential as:

$$e^{-n \mathcal{A}(B(x, r) \cup B(x', r'))} = e^{-n\pi(r^2 + r'^2)} + \left( e^{-n \mathcal{A}(B(x, r) \cup B(x', r'))} - e^{-n\pi(r^2 + r'^2)} \right)$$

and applying Fubini's theorem, we get:

$$\mathbb{E} \left[ \frac{1}{4} \sum_{p_1 \neq, 4 \in X_n^4} \ell_{VP_{X_n}}(p_{1..2}) \ell_{VP_{X_n}}(p_{3..4}) \right] \leq \mathbb{E} [\ell(VP_{X_n})]^2 + r_n,$$

where

$$r_n = \frac{n^4}{4} \int_{[0,1]^2} \int_{\mathbb{R}_{\geq 0}^2} \int_{[0,2\pi]^4} \left( e^{-n\mathcal{A}(B(x,r)\cup B(x',r'))} - e^{-n\pi(r^2+r'^2)} \right) 2r \left| \sin \frac{\alpha_1 - \alpha_2}{2} \right| \\ 2r' \left| \sin \frac{\alpha_3 - \alpha_4}{2} \right| r^2 |\cos \alpha_2 - \cos \alpha_1| r'^2 |\cos \alpha_4 - \cos \alpha_3| d\alpha_{1..4} dr dr' dx dx'.$$

Breaking the symmetry between  $r$  and  $r'$ , we get

$$r_n = 2n^4 \int_{[0,1]^2} \int_{\mathbb{R}_{\geq 0}^2} \int_{r'}^{\infty} \left( e^{-n\mathcal{A}(B(x,r)\cup B(x',r'))} - e^{-n\pi(r^2+r'^2)} \right) r^3 r'^3 dr dr' dx dx' \\ \times \int_{[0,2\pi]^4} \left| \sin \frac{\alpha_1 - \alpha_2}{2} \sin \frac{\alpha_3 - \alpha_4}{2} (\cos \alpha_2 - \cos \alpha_1) (\cos \alpha_4 - \cos \alpha_3) \right| d\alpha_{1..4} \\ = 2n^4 \int_{[0,1]^2} \int_{\mathbb{R}_{\geq 0}^2} \int_{r'}^{\infty} \left( e^{-n\mathcal{A}(B(x,r)\cup B(x',r'))} - e^{-n\pi(r^2+r'^2)} \right) r^3 r'^3 dr dr' dx dx' \times (8\pi)^2.$$

Since we now have  $r' \leq r$ , we get

$$\left( e^{-n\mathcal{A}(B(x,r)\cup B(x',r'))} - e^{-n\pi(r^2+r'^2)} \right) \leq e^{-n\pi r^2}.$$

Noticing that the integral on  $\alpha_{1..4}$  is the square of the one in Equation (1),  $r_n$  can be bounded:

$$r_n \leq 2(8\pi)^2 n^4 \int_{[0,1]^2} \int_0^{\infty} \int_0^r r^6 e^{-n\pi r^2} \mathbb{1}_{[B(x,r)\cap B(x',r') \neq \emptyset]} dr' dr dx dx' \\ \leq 128\pi^2 n^4 \int_0^1 \int_{x'-2r}^{x'+2r} \int_0^{\infty} r^7 e^{-n\pi r^2} dr dx dx' \\ \leq 128\pi^2 n^4 \int_0^{\infty} 4r^8 e^{-n\pi r^2} dr \\ \leq 128\pi^2 n^4 \cdot 4 \frac{105}{32\pi^4 n^4 \sqrt{n}} = O(n^{-\frac{1}{2}}).$$

The first term of Equation (2) can be computed exactly and proves the lower bound on the variance (since all three terms are trivially positives):

$$\mathbb{E} \left[ \sum_{p_1 \neq p_2 \in X_n^2} \ell_{VP_{X_n}}(p_{1..2})^2 \right] \\ = n^2 \int_{(\mathbb{R}^2)^2} \mathbb{E} \left[ \mathbb{1}_{[B(p_1, p_2) \cap X_n = \emptyset]} \mathbb{1}_{[M(p_1, p_2) \in [st)]} \|p_1 p_2\|^2 \right] dp_1 dp_2 \\ = n^2 \int_0^1 \int_0^{\infty} \int_{[0,2\pi]^2} e^{-n\pi r^2} 4r^2 \sin^2 \frac{\alpha_1 - \alpha_2}{2} r^2 |\cos \alpha_1 - \cos \alpha_2| d\alpha_1 d\alpha_2 dr dx \\ = 4n^2 \int_0^1 dx \int_0^{\infty} e^{-n\pi r^2} r^4 dr \int_{[0,2\pi]^2} \sin^2 \frac{\alpha_1 - \alpha_2}{2} |\cos \alpha_1 - \cos \alpha_2| d\alpha_1 d\alpha_2 \\ = 4n^2 \frac{3}{4\pi n^{\frac{5}{2}}} \frac{16}{3} = \Theta(n^{-\frac{1}{2}}).$$

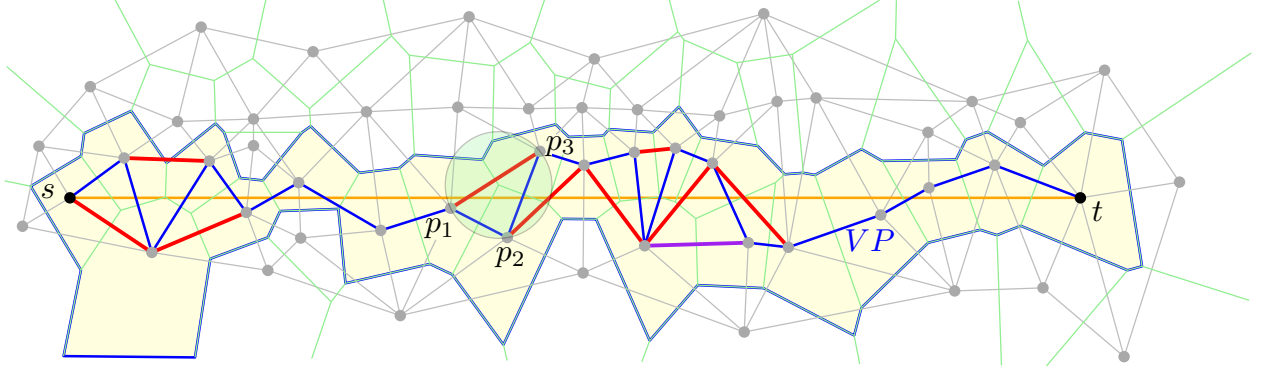


Figure 2: Shortcuts in Voronoi path of Figure 1. The shortcutting edge of triangular shortcuts are in red, the purple edge correspond to a quadrangular shortcut.

The second term of Equation (2) gives:

$$\begin{aligned}
& \mathbb{E} \left[ \sum_{p_1 \neq p_2, p_3 \in X_n^3} \ell_{VP_{X_n}}(p_1, p_2) \ell_{VP_{X_n}}(p_2, p_3) \right] \\
& \leq n^3 \int_{(\mathbb{R}^2)^3} \mathbb{E} \left[ \mathbb{1}_{[B(p_1, p_2) \cap X_n = \emptyset]} \mathbb{1}_{[B(p_2, p_3) \cap X_n = \emptyset]} \mathbb{1}_{[M(p_1, p_2) \in [st]]} \mathbb{1}_{[M(p_2, p_3) \in [st]]} \|p_1 p_2\| \|p_2 p_3\| \right] \\
& \quad dp_1 dp_2 dp_3 \\
& \leq 2n^3 \int_{(\mathbb{R}^2)^3} e^{-n\pi R(p_1, p_2)^2} \mathbb{1}_{[\|p_2 p_3\| \leq \|p_1 p_2\|]} \mathbb{1}_{[M(p_1, p_2) \in [st]]} \|p_1 p_2\| \|p_2 p_3\| dp_1 dp_2 dp_3 \\
& \leq 2n^3 \int_{(\mathbb{R}^2)^3} e^{-n\pi R(p_1, p_2)^2} \mathbb{1}_{[p_3 \in B(M(p_1, p_2), 3R(p_1, p_2))]} \mathbb{1}_{[M(p_1, p_2) \in [st]]} 4R(p_1, p_2)^2 dp_1 dp_2 dp_3 \\
& = 8n^3 \int_{(\mathbb{R}^2)^2} e^{-n\pi R(p_1, p_2)^2} 9\pi R(p_1, p_2)^2 \mathbb{1}_{[M(p_1, p_2) \in [st]]} R(p_1, p_2)^2 dp_1 dp_2 \\
& = 72\pi n^3 \int_0^1 dx \int_0^\infty e^{-n\pi r^2} r^2 r^2 dr \int_{[0, 2\pi]^2} |\cos \alpha_2 - \cos \alpha_1| d\alpha_2 d\alpha_1 \\
& \leq 72\pi n^3 \cdot \frac{15}{16\pi^3 n^{\frac{7}{2}}} \cdot 8 = O(n^{-\frac{1}{2}}).
\end{aligned}$$

Combining the three terms of Equation (2) yields the upper bound on the variance.  $\square$

## 5 Improving the Voronoi Path

We call shortcut of  $VP_\chi$  a triangle  $(p_1, p_2, p_3)$  such that  $[p_1 p_2]$  and  $[p_2 p_3]$  are in the Voronoi Path, and  $(p_1, p_2, p_3)$  is a triangle in  $\text{Del}(\chi)$  (see red edges in Figure 2).

Notice that there may exist other shortcuts replacing more than two edges in the Voronoi path (e.g., the purple edge in Figure 2) but the probability of existence decrease with the length of the replaced chain. In this paper we limit our interest to the triangular shortcuts.

Let  $\ell_{SC}(p_1, p_2, p_3)$  be defined as the length saved by taking the shortcut  $(p_1, p_2, p_3)$ , i.e  $\ell_{SC}(p_1, p_2, p_3) = \|p_1 p_2\| + \|p_2 p_3\| - \|p_1 p_3\|$ .

As shown in Figure 2 some shortcuts are incompatible, but the set of shortcuts can be divided in two subsets: the shortcuts above the Voronoi path and the shortcuts below the Voronoi path. It is easy to observe



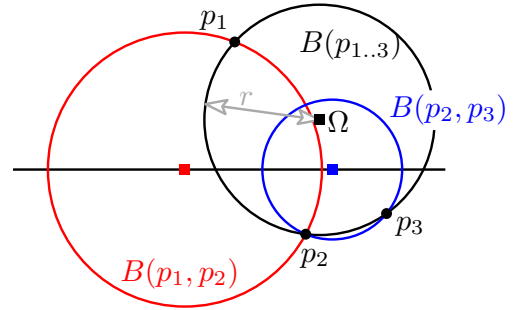
that the shortcuts in the same subset are compatible. By symmetry, the expected length of the shortcuts above the Voronoi path is equal to the one of shortcuts below the Voronoi path and is equal to half the total length of all shortcuts. Let  $gain_{X_n}$  denote this expected saving in the Voronoi path for a Poisson point process  $X_n$  considering only the shortcuts above the Voronoi path. We have:

$$\mathbb{E}[gain_{X_n}] = \mathbb{E} \left[ \frac{1}{2} \sum_{p_1 \neq, 3 \in X_n^3} \mathbb{1}_{[p_1..3 \in \text{Del}(X_n)]} \mathbb{1}_{[p_1..2 \in VP_{X_n}]} \mathbb{1}_{[p_2..3 \in VP_{X_n}]} \mathbb{1}_{[x_{p_1} < x_{p_2} < x_{p_3}]} \mathbb{1}_{[(p_1, p_2, p_3) \text{ ccw}]} \ell_{SC}(p_1..3) \right],$$

where ccw is a shorthand for counterclockwise. We use the Slivnyak-Mecke formula:

$$\begin{aligned} \mathbb{E}[gain_{X_n}] &= \frac{n^3}{2} \int_{(\mathbb{R}^2)^3} \mathbb{E} \left[ \mathbb{1}_{[p_1..3 \in \text{Del}(X_n \cup \{p_1..3\})]} \mathbb{1}_{[p_1..2 \in VP_{X_n \cup \{p_3\}}]} \mathbb{1}_{[p_2..3 \in VP_{X_n \cup \{p_1\}}]} \right. \\ &\quad \left. \mathbb{1}_{[x_{p_1} < x_{p_2} < x_{p_3}]} \mathbb{1}_{[(p_1, p_2, p_3) \text{ ccw}]} \ell_{SC}(p_1..3) \right] dp_{1..3} \\ &= \frac{n^3}{2} \int_{(\mathbb{R}^2)^3} \mathbb{P}[(B(p_1..3) \cup B(p_1, p_2) \cup B(p_2, p_3)) \cap X_n = \emptyset] \\ &\quad \mathbb{1}_{[M(p_1, p_2) \in [st]]} \mathbb{1}_{[M(p_2, p_3) \in [st]]} \mathbb{1}_{[p_1 \notin B(p_2, p_3)]} \mathbb{1}_{[p_3 \notin B(p_1, p_2)]} \\ &\quad \mathbb{1}_{[x_{p_1} < x_{p_2} < x_{p_3}]} \mathbb{1}_{[(p_1, p_2, p_3) \text{ ccw}]} \ell_{SC}(p_1..3) dp_{1..3}. \end{aligned}$$

The assumption  $x_{p_1} < x_{p_2} < x_{p_3}$  ensure that each triangle is counted only once. Amongst the shortcuts, we consider only the shortcuts with  $y_\Omega > 0 > y_{p_2}$  (with  $\Omega$  the center of  $B(p_1..3)$ ) and  $p_1, p_2, p_3$  counterclockwise then  $p_1 \notin B(p_2, p_3)$  and  $p_3 \notin B(p_1, p_2)$ . Since we neglect some



shortcuts, in the sequel, we only have a lower bound on  $gain_{X_n}$ :

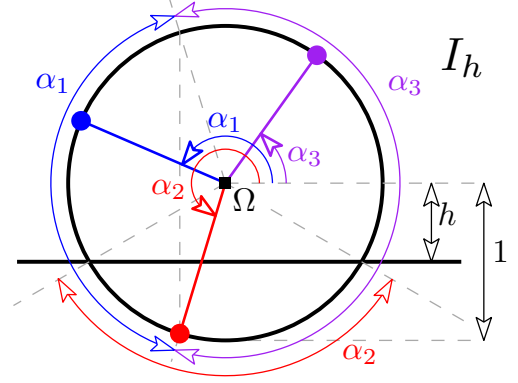
$$\begin{aligned} \mathbb{E}[gain_{X_n}] &\geq n^3 \int_{(\mathbb{R}^2)^3} e^{-n \mathcal{A}(B(p_1..3) \cup B(p_1, p_2) \cup B(p_2, p_3))} \mathbb{1}_{[M(p_1, p_2) \in [st]]} \mathbb{1}_{[M(p_2, p_3) \in [st]]} \mathbb{1}_{[y_{p_2} < 0]} \\ &\quad \mathbb{1}_{[y_\Omega > 0]} \mathbb{1}_{[x_{p_1} < x_{p_2} < x_{p_3}]} \mathbb{1}_{[(p_1, p_2, p_3) \text{ ccw}]} \ell_{SC}(p_1..3) dp_{1..3} = E_1. \end{aligned}$$

The end of this section is devoted to the computation of the above integral. Unfortunately, we do not succeed to compute it symbolically. We will reorganize the factors, substitute variables and make some symbolic integration to obtain some trigonometric integral that we will compute numerically.

Let  $r$  be the radius of  $B(p_{1..3})$ ,

$$S\left(\frac{y_\Omega}{r}, \alpha_1, \alpha_2, \alpha_3\right) = \frac{\mathcal{A}(B(p_{1..3}) \cup B(p_1, p_2) \cup B(p_2, p_3))}{r^2}$$

be the area of the union of the three balls normalized by  $r^2$ , and  $h = \frac{y_\Omega}{r}$  the normalized distance from  $\Omega$  to line  $(st)$ . Since  $\Omega$  is assumed above line  $(st)$  and  $p_2$  below it,  $h \in [0, 1]$ . We define an integration domain for the angles  $\alpha_i$ :



$$I_h = \left\{ (\alpha_1, \alpha_2, \alpha_3) \in \mathbb{R}^3 \begin{cases} 2\pi - \alpha_2 < \alpha_1 < \alpha_2 \\ \pi + \arcsin h < \alpha_2 < 2\pi - \arcsin h \\ \alpha_2 - 2\pi < \alpha_3 < 2\pi - \alpha_2 \end{cases} \right\}.$$

$E_1$  becomes:

$$E_1 = n^3 \int_{(\mathbb{R}^2)^3} e^{-nr^2 S\left(\frac{y_\Omega}{r}, \alpha_1, \alpha_2, \alpha_3\right)} \mathbb{1}_{[M(p_1, p_2) \in [st]]} \mathbb{1}_{[M(p_2, p_3) \in [st]]} \mathbb{1}_{[0 < y_\Omega < r]} \mathbb{1}_{[\alpha_{1..3} \in I_h]} \ell_{SC}(p_{1..3}) dp_{1..3}.$$

Basic trigonometry gives:  $x_{M(p_1, p_2)} = x_\Omega - \frac{y_\Omega}{\tan(\frac{\alpha_1 + \alpha_2}{2})}$  and  $x_{M(p_2, p_3)} = x_\Omega - \frac{y_\Omega}{\tan(\frac{\alpha_2 + \alpha_3}{2})}$ . Defining

$$J_{y_\Omega, \alpha_{1..3}} = \begin{cases} \left[ \frac{y_\Omega}{\tan(\frac{\alpha_1 + \alpha_2}{2})}, 1 + \frac{y_\Omega}{\tan(\frac{\alpha_2 + \alpha_3}{2})} \right] & , \text{ if } \frac{y_\Omega}{\tan(\frac{\alpha_1 + \alpha_2}{2})} \leq 1 + \frac{y_\Omega}{\tan(\frac{\alpha_2 + \alpha_3}{2})} , \\ \emptyset & , \text{ otherwise} \end{cases}$$

we have  $\mathbb{1}_{[M(p_1, p_2) \in [st]]} \mathbb{1}_{[M(p_2, p_3) \in [st]]} = \mathbb{1}_{[x_\Omega \in J_{y_\Omega, \alpha_{1..3}}]}$ . We are now ready to substitute the variables using the Blaschke-Petkantschin formula. We get:

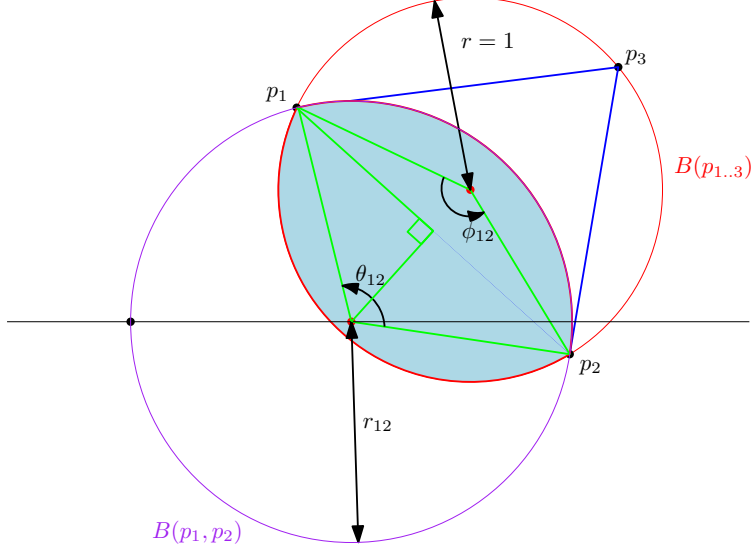
$$\begin{aligned} E_1 &= n^3 \int_{[0, 2\pi]^3} \int_0^\infty \int_{\mathbb{R}} \int_{\mathbb{R}} e^{-nr^2 S\left(\frac{y_\Omega}{r}, \alpha_1, \alpha_2, \alpha_3\right)} \mathbb{1}_{[x_\Omega \in J_{y_\Omega, \alpha_{1..3}}]} \mathbb{1}_{[0 < y_\Omega < r]} \mathbb{1}_{[\alpha_{1..3} \in I_h]} \\ &\quad 2r \left( \left| \sin \frac{\alpha_1 - \alpha_2}{2} \right| + \left| \sin \frac{\alpha_2 - \alpha_3}{2} \right| - \left| \sin \frac{\alpha_1 - \alpha_3}{2} \right| \right) 2r^3 \mathcal{A}(\alpha_{1..3}) dy_\Omega dx_\Omega dr d\alpha_{1..3}, \\ &= 2n^3 \int_{[0, 2\pi]^3} \int_0^\infty \int_0^r \left( \int_{J_{y, \alpha_{1..3}}} dx \right) e^{-nr^2 S\left(\frac{y}{r}, \alpha_1, \alpha_2, \alpha_3\right)} \mathbb{1}_{[\alpha_{1..3} \in I_h]} \\ &\quad g(\alpha_{1..3}) r^4 dy dr d\alpha_{1..3}, \end{aligned}$$

where  $g(\alpha_{1..3}) = 2 \mathcal{A}(\alpha_{1..3}) \left( \left| \sin \frac{\alpha_1 - \alpha_2}{2} \right| + \left| \sin \frac{\alpha_2 - \alpha_3}{2} \right| - \left| \sin \frac{\alpha_1 - \alpha_3}{2} \right| \right)$ ,

$$E_1 \geq 2n^3 \int_{[0, 2\pi]^3} \int_0^1 \int_0^\infty (1 - rh g'(\alpha_{1..3})) e^{-nr^2 S(h, \alpha_1, \alpha_2, \alpha_3)} r^5 \mathbb{1}_{[\alpha_{1..3} \in I_h]} g(\alpha_{1..3}) dr dh d\alpha_{1..3},$$

where  $g'(\alpha_{1..3}) = \frac{1}{\tan(\frac{\alpha_1 + \alpha_2}{2})} - \frac{1}{\tan(\frac{\alpha_2 + \alpha_3}{2})}$ . The length of  $J_{y, \alpha_{1..3}}$  is  $1 - rh g'(\alpha_{1..3})$  when the interval is nonempty; otherwise,  $1 - rh g'(\alpha_{1..3})$  is negative and still bounds the interval's length from below.

Since  $n^3 \int_0^\infty e^{-nr^2 S(h, \alpha_1, \alpha_2, \alpha_3)} r^6 dr = O\left(n^{-\frac{1}{2}}\right)$  the contribution of the term  $rhg'$  to  $E_1$  is negligible and



we get

$$\begin{aligned}
E_1 &\geq 2n^3 \int_{[0,2\pi]^3} \int_0^1 \left( \int_0^\infty e^{-nr^2 S(h, \alpha_1, \alpha_2, \alpha_3)} r^5 dr \right) \mathbb{1}_{[\alpha_{1..3} \in I_h]} g(\alpha_{1..3}) dh d\alpha_{1..3} + O\left(n^{-\frac{1}{2}}\right) \\
&= 2n^3 \int_{[0,2\pi]^3} \int_0^1 \left( \frac{1}{n^3 S(h, \alpha_1, \alpha_2, \alpha_3)^3} \right) \mathbb{1}_{[\alpha_{1..3} \in I_h]} g(\alpha_{1..3}) dh d\alpha_{1..3} + O\left(n^{-\frac{1}{2}}\right) \\
&= 2 \int_0^1 \int_{I_h} \frac{g(\alpha_{1..3})}{S(h, \alpha_1, \alpha_2, \alpha_3)^3} d\alpha_{1..3} dh + O\left(n^{-\frac{1}{2}}\right). \tag{3}
\end{aligned}$$

### Determination of $S(h, \alpha_1, \alpha_2, \alpha_3)$

$$S(h, \alpha_1, \alpha_2, \alpha_3) = \mathcal{A}(B(u_{1..3}) \cup B(u_1, u_2) \cup B(u_2, u_3))$$

with  $u_i = (\cos \alpha_i, \sin \alpha_i)$ .

$$\begin{aligned}
S(h, \alpha_1, \alpha_2, \alpha_3) &= \mathcal{A}(B(u_{1..3})) + \mathcal{A}(B(u_1, u_2)) + \mathcal{A}(B(u_2, u_3)) \\
&\quad - \mathcal{A}(B(u_{1..3}) \cap B(u_1, u_2)) - \mathcal{A}(B(u_{1..3}) \cap B(u_2, u_3)) \\
&\quad - \mathcal{A}(B(u_1, u_2) \cap B(u_2, u_3)) + \mathcal{A}(B(u_{1..3}) \cap B(u_1, u_2) \cap B(u_2, u_3)).
\end{aligned}$$

We will look at the different terms of this sum. First we remark that when  $\alpha_{1..3} \in I_h$ , the two last terms disappear since  $B(u_1, u_2) \cap B(u_2, u_3) \subset B(u_{1..3})$  (the apexes of  $B(u_1, u_2) \cap B(u_2, u_3)$  are  $p_2$  and its symmetric with respect to the line  $y = -h$ ).

The first term is just  $\pi$  the area of the unit circle.

The second and third terms are  $\pi r_{12}^2$  and  $\pi r_{23}^2$  with  $r_{12} = R(u_1, u_2)$  and  $r_{23} = R(u_2, u_3)$ .

The fourth term is

$$\mathcal{A}(B(u_{1..3}) \cap B(u_1, u_2)) = \frac{1}{2} r_{12}^2 (\theta_{12} - |\sin \theta_{12}|) + \frac{1}{2} (\phi_{12} - |\sin \phi_{12}|),$$

with  $\phi_{12} = \widehat{p_1 \Omega p_2}$  and  $\theta_{12} = \widehat{p_2 M(p_1, p_2) p_1}$  the angles under which  $p_1 p_2$  is viewed from  $\Omega$  and  $M(p_1, p_2)$ .

The fifth term is similar to the fourth one.

Above undefined quantities can be expressed in term of  $h$  and  $\alpha_{1..3}$ . Since the angle of  $\Omega M(u_1, u_2)$  is  $\frac{\pi}{2} - \frac{\alpha_1 + \alpha_2}{2}$  and  $y_{M(u_1, u_2)} = -h$  we have  $x_{M(u_1, u_2)} = -h \tan \frac{\pi + \alpha_1 + \alpha_2}{2}$ . We deduce  $r_{12}^2 = (\sin \alpha_2 + h)^2 + (\cos \alpha_2 + h \tan \frac{\pi + \alpha_1 + \alpha_2}{2})^2$ .

Similarly  $r_{23}^2 = (\sin \alpha_2 + h)^2 + (\cos \alpha_2 + h \tan \frac{\pi + \alpha_3 + \alpha_2}{2})^2$ .

The angles  $\phi$  are easy to compute:  $\phi_{12} = \alpha_2 - \alpha_1$  and  $\phi_{23} = \alpha_3 - \alpha_2 + 2\pi$ .

The angle  $\theta_{12}$  verifies

$$|\cos \frac{\theta_{12}}{2}| = \frac{\|M(u_1, u_2) \frac{u_1 + u_2}{2}\|}{r_{12}} = \frac{\sqrt{r_{12}^2 - \frac{\|u_1 u_2\|}{2}}}{r_{12}} = \sqrt{1 - \left(\frac{\sin \frac{\alpha_1 - \alpha_2}{2}}{r_{12}}\right)^2},$$

$\cos \frac{\theta_{12}}{2} \geq 0$  iff  $0 \leq 2h + \sin \alpha_1 + \sin \alpha_2$ , thus

$$\theta_{12} = 2 \arccos \left( \sqrt{1 - \left(\frac{\sin \frac{\alpha_1 - \alpha_2}{2}}{r_{12}}\right)^2} \operatorname{sign}(2h + \sin \alpha_1 + \sin \alpha_2) \right).$$

By a very similar reasoning we get

$$\theta_{23} = 2 \arccos \left( \sqrt{1 - \left(\frac{\sin \frac{\alpha_2 - \alpha_3}{2}}{r_{23}}\right)^2} \operatorname{sign}(2h + \sin \alpha_2 + \sin \alpha_3) \right).$$

## Value of the gain

Using the above expression for  $S(h, \alpha_{1..3})$ , the integral of Equation (3) has been numerically approximated using Maple giving  $\mathbb{E}[gain_{X_n}] \simeq 0.108$ . So the expectation of the length of the new path is 1.165. Notice that expression in Equation (3) is the well defined integral of a positive function independent of any parameters, thus it is clearly a positive constant. Maple file with these computation is available with the preprint of this paper.[9]

## 6 Concluding remarks

As a concluding remark, we mention several possibilities of paths from  $s$  to  $t$  that can be defined in a Delaunay triangulation: the shortest path, the compass route (vertex following  $v$  is the one minimizing the angle with  $vt$ ), upper path (edges  $vw$  of triangles  $uvw$  with  $u$  below line  $(st)$  and  $v$  and  $w$  above), the closest neighbor path (vertex following  $v$  is the neighbor of  $v$  minimizing the distance to  $t$ ), the Voronoi path (VP), the Voronoi path with all possible shortcuts taken greedily, and the Voronoi path with the ccw shortcuts (as in Section 5).

Some of these paths are locally defined, i.e., the fact that  $vw$  belongs to the path can be decided knowing only  $s$ ,  $t$  and some neighborhood of  $vw$ . Some are incremental, i.e., the vertex following  $v$  can be decided knowing that  $v$  is on the path,  $s$ ,  $t$ , and some neighborhood of  $v$ .

Using CGAL[6], we compute the length of these paths for random set of points. The length and the number of edges reported have been obtained averaging over 1000 experiments with point density  $10^6$ .

Path	Experimental Length	Number of edges	Path properties	Theoretical bound	Ref
Shortest path	1.041	927		$\in [1 + 10^{-11}, 1.182]$	[7]
Compass route	1.068	956	incremental	$\Theta(\sqrt{n})$ edges	[8]
Voronoi Path greedy shortcuts	1.130	995	incremental		
Voronoi Path ccw shortcuts	1.164	1081	incremental locally defined	using numerical integration 1.165	
Closest neighbor walk	1.167	873	incremental	$\Theta(\sqrt{n})$ edges	[8]
Upper path	1.177	1072	incremental locally defined	$\frac{35}{3\pi^2} \simeq 1.182$	[7]
Voronoi Path	1.274	1273	incremental locally defined	$\frac{4}{\pi} \simeq 1.273$	[1]

In a companion paper[5]

we prove that the expected length of the Voronoi path between two points at unit distance increases with the dimension from about  $\frac{3}{2}$  in 3D to  $\Theta\left(\sqrt{\frac{2d}{\pi}}\right)$  when  $d \rightarrow \infty$ . Analyzing the shortcuts in higher dimension with the tools in the current paper seems out of reach.

## References

- [1] François Baccelli, Konstantin Tchoumatchenko, and Sergei Zuyev. Markov paths on the Poisson-Delaunay graph with applications to routing in mobile networks. *Adv. in Appl. Probab.*, 32(1):1–18, 2000. doi:10.1239/aap/1013540019.
- [2] Prosenjit Bose and Luc Devroye. On the stabbing number of a random Delaunay triangulation. *Computational Geometry: Theory and Applications*, 36:89–105, 2006. doi:10.1016/j.comgeo.2006.05.005.
- [3] Prosenjit Bose and Pat Morin. Online routing in triangulations. *SIAM Journal on Computing*, 33:937–951, 2004. doi:10.1137/S0097539700369387.
- [4] Nicolas Broutin, Olivier Devillers, and Ross Hemsley. Efficiently navigating a random Delaunay triangulation. *Random Structures and Algorithms*, page 46, 2016. URL: <https://hal.inria.fr/hal-00940743>, doi:10.1002/rsa.20630.
- [5] Pedro Machado Manhães De Castro and Olivier Devillers. Expected length of the Voronoi path in a high dimensional Poisson-Delaunay triangulation. *Discrete and Computational Geometry*, pages 1–20, 2017. URL: <https://hal.inria.fr/hal-01477030>, doi:10.1007/s00454-017-9866-y.
- [6] Computational Geometry Algorithms Library. URL: <http://www.cgal.org>.
- [7] Nicolas Chenavier and Olivier Devillers. Stretch factor in a planar Poisson-Delaunay triangulation with a large intensity. *Advances in Applied Probability*, 50(1), 2018. URL: <https://hal.inria.fr/hal-01700778>.
- [8] Olivier Devillers and Ross Hemsley. The worst visibility walk in a random Delaunay triangulation is  $O(\sqrt{n})$ . *Journal of Computational Geometry*, 7(1):332–359, 2016. URL: <https://hal.inria.fr/hal-01348831>.
- [9] Olivier Devillers and Louis Noizet. Walking in a Planar Poisson-Delaunay Triangulation: Shortcuts in the Voronoi Path. Research Report RR-8946, INRIA Nancy, August 2016. URL: <https://hal.inria.fr/hal-01353585>.
- [10] Olivier Devillers, Sylvain Pion, and Monique Teillaud. Walking in a Triangulation. *International Journal of Foundations of Computer Science*, 13:181–199, 2002. URL: <https://hal.inria.fr/inria-00102194>.
- [11] Luc Devroye, Christophe Lemaire, and Jean-Michel Moreau. Expected time analysis for Delaunay point location. *Computational Geometry: Theory and Applications*, 29:61–89, 2004. doi:10.1016/j.comgeo.2004.02.002.
- [12] Rolf Schneider and Wolfgang Weil. *Stochastic and Integral Geometry*. Probability and Its Applications. Springer, 2008.